In Vitro Cell. Dev. Biol.—Animal 42:189–200, July–August 2006

1071-2690/06 $18.00+0.00

STRATEGY FOR THE DEVELOPMENT OF A MATCHED SET OF TRANSPORT-COMPETENT, ANGIOTENSIN RECEPTOR–DEFICIENT PROXIMAL TUBULE CELL LINES

PHILIP G. WOOST,[1] ROBERT J. KOLB, MARGARET FINESILVER, IRENE MACKRAJ, HANS IMBODEN, THOMAS M. COFFMAN, AND ULRICH HOPFER

Department of Physiology and Biophysics, Case Western Reserve University, Cleveland, Ohio 44106 (P. G. W., M. F., U. H.), Brigham and Women's Hospital, Harvard Medical School, 4 Blackfan Circle, Room 520, Boston, Massachusetts 02115 (R. J. K.), Department of Human Physiology and Physiological Chemistry, School of Basic and Applied Medical Sciences, University of Durban-Westville, Private Bag X54001, Durban, 4001 South Africa (I. M.), Institute of Zoology, University of Berne, Baltzerstrasse 6, 3012 Berne, Switzerland (H. I.), and Department of Medicine-Nephrology, Duke University and Durham Veterans Affair Medical Centers, Durham, North Carolina 27705 (T. M. C.)

(Received 1 November 2005; accepted 11 May 2006)

SUMMARY

In the proximal convoluted tubule (PCT) angiotensin II (Ang II) modulates fluid and electrolyte transport through at least two pharmacologically distinct receptor subtypes: AT_1 and AT_2. Development of cell lines that lack these receptors are potentially useful models to probe the complex cellular details of Ang II regulation. To this end, angiotensin receptor–deficient mice were bred with an Immortomouse®, which harbors a thermolabile SV40 large-T antigen (Tag). S1 PCT segments from kidneys of F_2 mice were microdissected, placed in culture, and maintained under conditions that enhanced cell growth, i.e., promoted Tag expression and thermostability. Three different types of angiotensin receptor–deficient cell lines, (AT_{1A} [−/−], Tag [+/−]), (AT_{1B} [−/−], Tag [+/−]), and (AT_{1A} [−/−], AT_{1B} [−/−], Tag [+/+]), as well as wild type cell lines were generated. Screening and characterization, which were conducted under culture conditions that promoted cellular differentiation, included: measurements of transepithelial transport, such as basal monolayer short-circuit current (Isc; −3 to 3 μA/cm²), basal monolayer conductance (G, 2 to 10 mS/cm²), Na_3^+–phosphate cotransport (ΔIsc of 2 to 3 μA/cm² at 1 m*M*), and Na_3^+–succinate cotransport (ΔIsc of 1 to 9 μA/cm² at 2 m*M*). Morphology of cell monolayers showed an extensive brush border, well-defined tight junctions, and primary cilia. Receptor functionality was assessed by Ang II–stimulated β-arrestin 2 translocation and showed an Ang II–mediated response in wild type but not (AT_{1A} [−/−], AT_{1B} [−/−]) cells. Cell lines were amplified, yielding a virtually unlimited supply of highly differentiated, transport-competent, angiotensin receptor–deficient PCT cell lines.

Key words: cilium; electrolyte transport; epithelial cell line; Immortomouse®; proximal tubule; SV40 large T-antigen.

INTRODUCTION

In vitro cell models are potentially useful and important research tools to probe complex biological questions at the cellular and molecular levels. Yet, meaningful and coherent strategies leading to the development and maintenance of established cell lines are lacking or missing altogether. Over the course of the last decade our laboratory has been involved in the development and study of renal epithelial cell lines (Romero et al., 1992; Woost et al.; 1996; Orosz et al., 2004). During that time application of known cell biology and improved cell culture technology has led to a four-point strategy: cell line initiation, screening, expansion-differentiation, and characterization. We exploited this strategy in the present study as we describe the development of Ang II receptor–deficient PCT cell lines.

The multifunctional peptide hormone Ang II is the major biologically active product of the renin-angiotensin system and an important modulator of cardiovascular homeostasis, systemic blood pressure, and renal function. At least two pharmacologically distinct receptor subtypes mediate the biological actions of Ang II: AT_1 (in rodents, AT_{1A} and AT_{1B}) and AT_2. Both are G protein–coupled receptors (also called 7 transmembrane receptors [7TMRs]). AT_1 receptors, which are widely distributed in several adult tissues, including the kidney, initiate many of the well-characterized actions of Ang II, such as vasoconstriction, aldosterone release, and stimulation of cellular growth. While AT_2 receptors are expressed abundantly during fetal development and are less numerous in normal adult tissues, they nevertheless appear to play an important physiological role in adult tissue and are thought to mediate vasodilatation, apoptosis, and some aspects of cellular differentiation. More specifically, in the PCT Ang II regulates fluid and electrolyte transport, including Na^+, Cl^-, HCO_3^-, and water reabsorption. (For reviews, *see* Inagami, 1999; de Gasparo et al., 2000; Quan and Baum, 2000; Dinh et al., 2001).

A number of important advances have been made in recent years, including expression cloning of the various Ang-R subtypes, generation of receptor-deficient (knock-out) mice (Ichiki et al., 1995; Ito et al., 1995; Oliverio et al., 1998; Oliverio and Coffman, 2000),

[1] To whom correspondence should be addressed at Department of Physiology and Biophysics, Case Western Reserve University, 10900 Euclid Avenue, Cleveland, Ohio 44106-4970. E-mail: philip.woost@case.edu

and the ongoing elucidation of receptor-mediated signal transduction pathways (Touyz and Berry, 2002). Despite these advances, the cellular mechanisms underlying many of the biological effects associated with Ang II in the proximal tubule and elsewhere remain unclear. For example, polarization of the microtubule cytoskeleton (du Cheyron et al., 2003; Kolb et al., 2004), regulation of the intratubular renin-angiotensin system (Navar et al., 1997), trafficking of receptors and transporters to apical and basolateral plasma membranes (du Cheyron et al., 2003; Kolb et al., 2004), collection of apical microtubule-dependent membrane proteins in condensed apical recycling endosomes in the proximity of the cilium (Kolb et al., 2004), and other Ang II–mediated effects warrant more research. A well-defined, well-characterized experimental paradigm is critical and, perhaps, is most easily addressed at the cellular level by a cell culture system.

The utility of in vitro cell models, however, is often underappreciated. Yet, well-differentiated epithelial cell models allow the integration of apical and basolateral fluxes, hormones and cell behavior, transport and metabolism, and function and morphology. Understanding and regulating the underlying mechanisms of differentiation represent a significant challenge. The usefulness of a given cell line is largely dependent on its degree of differentiation, the ability to maintain that state of differentiation, and whether or not that differentiation state is sufficient to address the question(s) being asked. While a given cell line may be a significant research tool, in the end, however, the ability to manipulate its growth and differentiation in culture is even more important. Only then is it suitable to precisely and accurately study issues of cellular integration and homeostasis.

In the last decade the methods for isolating cell lines, especially those that retain the differentiated features of parent cells, have dramatically improved (Hopfer et al., 1996). In particular, cell lines from transgenic mice harboring an immortalizing gene are a recent and important development (Jat et al., 1991). The commercially available Immortomouse® successfully carries a temperature-sensitive (tsA58) mutation in SV40 large Tag, which permits the conditional immortalization of cells in vitro (Jat et al., 1991). Breeding an Immortomouse® with a mouse that possesses a specific genetic trait yields some F_2 progeny that harbor both the immortalizing and targeted genes. In principle, any tissue from these select F_2 mice is a candidate for cell line development, provided the appropriate cell culture conditions have been established. Thus, it becomes possible to study the alteration of a particular gene on a specific cell type.

Here we describe the development of a virtually unlimited supply of early passage, highly differentiated, transport-competent proximal tubule cell lines that lack the AT_{1A}, AT_{1B}, or combined AT_{1A}/AT_{1B} receptors. We take advantage of recently developed Ang-R–deficient mice as well as the commercially available Immortomouse®. Although this work targeted the development of Ang-R–deficient proximal tubule cell lines, it is applicable to other tissues and cell types as well.

Materials and Methods

Mouse genotypes and husbandry. The development of Ang-R–deficient mice, i.e., *Agtr1a* (AT_{1A}) −/− and combined (*Agtr1a* [AT_{1A}] −/−, *Agtr1b* [AT_{1B}] −/−) mice, by gene targeting was described previously (Ito et al., 1995; Oliverio et al., 1998). (*Agtr1a* mice are commercially available from The Jackson Laboratory, Bar Harbor, ME.) Two male Immortomouse®s (homozygous for Tag) were purchased from Charles River Laboratories, Wilmington, MA. All mice shared a common C57BL/6 genetic background. The full-length cDNA for Tag was generously supplied by Dr. James W. Jacobberger's laboratory, Case Western Reserve University, Cleveland, OH.

Mice were bred and maintained in the Animal Resource Center at the School of Medicine, Case Western Reserve University, Cleveland, OH, in accordance with the Public Health Service Policy on Humane Care and Use of Laboratory Animals (National Institutes of Health, 2000). The experimental protocol was approved by the Institutional Animal Care and Use Committee, School of Medicine, Case Western Reserve University, Cleveland, OH. Mouse husbandry was accomplished using a polygamous mating scheme. Initially, a male Immortomouse® was housed with four female AT_{1A} (−/−) or combined (AT_{1A} [−/−], AT_{1B} [−/−]) mice per cage. Pregnant mice were isolated to their own cage prior to parturition, and offspring were weaned at 21 to 28 d. Mice of the F_1 generation were heterozygous for Tag as well as the targeted disruption in the AT_{1A} (−/−) or combined (AT_{1A} [−/−], AT_{1B} [−/−]) genes. When F_1 mice were approximately 8 to 9 wk old, mating continued by housing per cage one F_1 male with several F_1 female siblings. Following parturition and at the time of weaning, F_2 mice were lightly anesthetized with CO_2 (from dry ice) and a tail clip (0.5 cm) was taken for DNA purification and genotyping. Mating continued until F_2 mice of the desired genotype were obtained.

Genotyping. Genotyping was accomplished by restriction enzyme digestion of genomic DNA followed by Southern hybridization with probes that shared a common sequence in both wild type and targeted genes. The targeted construct was engineered by disrupting the Ang-R coding sequence with a neomycin (neo) cassette. Integration of the neo cassette introduced an additional restriction enzyme site, yielding a diagnostic fragment for the targeted, mutated allele, which was smaller in size compared with the wild type allele.

Plasmids containing hybridization probes for the various Ang-Rs (Ito et al., 1995; Oliverio et al., 1998) and Tag were amplified by conventional methods and then purified with Plasmid Maxi Kit (Qiagen Inc., Valencia, CA), according to the manufacturer's instructions. DNA probes were isolated following restriction enzyme digestion, agarose gel electrophoresis, and gel extraction (QIAquick Gel Extraction Kit [Qiagen Inc.]). The full-length cDNA was used as a probe for Tag. High molecular weight genomic DNA was isolated from tail clips using DNeasy Tissue Kit (Qiagen Inc.), according to the manufacturer's instructions.

Digoxigenin (DIG)-labeled DNA probes were used for Southern hybridization followed by chemiluminescent detection with an enzyme immunoassay, using DIG High Prime DNA Labeling and Detection Starter Kit II (Roche, Indianapolis, IN). Probe labeling and detection were performed according to the manufacturer's directions, with the following exception: a modified Church's Hybridization Buffer, composed of sodium phosphate (260 m*M*, pH 7.2), ethylenediaminetetraacetic acid, disodium salt (EDTA, 1 m*M*), lauryl sulfate, sodium salt (SDS, 7%), herring sperm DNA (0.3 mg/ml), and bovine serum albumin (2%), was used for hybridization and stringency washes at 58° C.

Microdissection, cell culture, and cryopreservation. Male or female 4- to 8-wk-old mice of the desired genotype were anesthetized with CO_2 (from dry ice), the aorta was clamped off below the kidneys, and their kidneys were perfused through the left ventricle with a modified Collin's preservative solution containing 140 m*M* D-glucose, 57 m*M* potassium phosphate, 15 m*M* KCl, 30 m*M* $MgSO_4 \cdot 7H_2O$, 10 m*M* $NaHCO_3$, 5 m*M* $NaHSO_3$, pH 7.25, and 5 U/ml heparin. Following complete blood washout, kidneys were excised, and superficial cortical slices were incubated in Hank's Balanced Salt Solution (HBSS; Life Technologies, Inc./GibcoBRL, Rockville, MD) containing 1 mg/ml collagenase (type IV; Sigma Chemical Co., St. Louis, MO) for 10 to 20 min at 37° C. Afterward, tissue slices were placed on ice and rinsed briefly in Renal Tubule Epithelial (RTE) medium composed of Dulbecco's Modified Eagle's Medium (DMEM; without glucose)/Ham's F-12 (1.8 g/l glucose), 1:1 (v/v); 10 n*M* aldosterone; 50 μ*M* L-ascorbic acid 2-phosphate; 4 μg/ml dexamethasone; 10 ng/ml epidermal growth factor (EGF); 5 g/ml insulin; 20 n*M* sodium selenite (Na_2SeO_3); 5 μg/ml transferrin; 1 n*M* L-3,3′,5-triiodothyronine (T_3); 15 m*M* HEPES; 1.2 mg/ml sodium bicarbonate ($NaHCO_3$), pH 7.4; and further supplemented with 100 U/ml penicillin G (pen) and 100 μg/ml streptomycin (strep). S1 segments of the PCT in RTE plus pen-strep were microdissected from the surrounding tissue in the following manner: The nephron was feathered apart with finely tipped forceps. The glomerulus was located. Then, a 1- to 2-mm portion of convoluted tubule was identified, isolated, and placed on a collagen-coated 12-mm culture plate insert (Millipore Corp., Bedford, MA).

Prior to microdissection, culture plate inserts were coated with 20% Eth-

icon collagen in 60% ethanol. (Ethicon collagen is a dispersion of mixed collagen types that was obtained from Ethicon Inc., a division of Johnson & Johnson [Somerville, NJ]). Collagen-coated inserts were allowed to air dry in a biological safety cabinet, and then irradiated with a UV light for 20 to 30 *min* to ensure sterility.

After placement on the insert, S1 segments were allowed to attach to the insert matrix by incubating in a minimal volume (50 to 100 μl) of RTE medium supplemented with pen-strep, 5% fetal bovine serum (FBS), and 10 U/ml recombinant mouse interferon-γ (IFN-γ) for 12 to 24 h at 33° C. After attachment, the volume of the apical chamber, i.e., the volume inside the insert, was increased to 130 to 150 μl RTE medium containing pen-strep, FBS, and IFN-γ, while the level of liquid in the basal chamber, i.e., the volume outside the insert, was maintained at the same height as the apical chamber, ensuring that the hydrostatic pressure between the two chambers was equal. When the insert was placed in a well of a 12-well culture plate, the volume of medium in the basal chamber was approximately 0.8 ml. In some cases after tissue attachment, cell outgrowth from proximal tubule segments was stimulated by co-culture with lethally irradiated (5000 to 6000 rads) NIH 3T3 fibroblasts. Irradiated fibroblasts were cultured on both the collagen-coated insert and underlying plastic well. Primary cultures were passaged with 0.05% trypsin and 0.53 m*M* EDTA in HBSS without Ca^{2+} or Mg^{2+} (trypsin-EDTA; Life Technologies, Inc./GibcoBRL) at a split ratio of 1:2 to 1:3.

Established cultures were routinely maintained at 33° C in a 5% CO_2 humidified atmosphere on 30-mm collagen-coated culture plate inserts in Expansion Medium (EM), i.e., RTE medium supplemented with 5% FBS and 10 U/ml IFN-γ. The expression and thermostability of Tag and thus cell growth and culture expansion were promoted by the presence of IFN-γ and the 33° C incubation temperature. Cultures were passaged with trypsin-EDTA at a split ratio of 1:5 to 1:10. In some experiments, cells were grown to confluency in EM, and then EM was replaced with Differentiation Medium (DM), a medium that was designed to promote cellular differentiation. DM was similar to EM, but lacks added the growth factors EGF, insulin, and interferon-γ on the basal side, and insulin, interferon-γ, and serum on the apical side. In addition, the incubation temperature was increased to 37° or 39° C, a labile temperature for Tag.

Following routine expansion and harvesting, cell lines were stored in liquid nitrogen in a cryopreservative solution. Cells were harvested with trypsin-EDTA, and then frozen in a solution composed of Cryoprotective Medium (Basal Eagle's Medium with HBSS and 15% dimethylsulfoxide without L-glutamine; BioWhittaker, Walkersville, MD) and RTE supplemented with 20% FBS (1:1, v/v). Vials were first stored at −70° C for 12 to 24 h and then transferred to liquid nitrogen.

RT-PCR of AT_{1A} and AT_{1B} mRNA. Total RNA or poly A^+ mRNA was isolated with RNeasy Mini Kit or Oligotex Direct mRNA Micro Kit (Qiagen Inc.), respectively. If necessary, contaminating genomic DNA was removed with DNA-free: DNase Treatment and Removal Reagents (Ambion Inc., Austin, TX). To discriminate between AT_{1A} and AT_{1B} mRNA, samples were analyzed as described by Zhu et al. (1998) with only minor modifications. Primers were sense (5′-CCAAAGTCACCTGCATCATC-3′) and antisense (5′-CACAATCGCCTAATTATCCTA-3′), and were common to both wild type genes, AT_{1A} and AT_{1B}. The sequence of the sense primer, however, lies within the region deleted in the mutated gene, and thus is absent from that gene, whereas the antisense sequence lies outside the deleted region and is maintained by both wild type and mutated genes. Reactions, using Qiagen OneStep Kit (Qiagen Inc.), included [Primer] = 0.8 μ*M*, annealing temperature = 55° C, and cycles = 35 to 45. Following RT-PCR, AT_{1A} was distinguished from AT_{1B} by digestion of 15 μl of the 50 μl reaction with 20 units *Eco*R1 (Roche). The 305-bp AT_{1A} amplification product yielded *Eco*R1 digestion products of 128 and 177 bp, whereas the AT_{1B} product was resistant to digestion. PCR and digestion products were separated on 2% agarose gels and visualized with ethidium bromide. In addition mRNA from combined (AT_{1A} [−/−], AT_{1B} [−/−]) cells was also probed for AT_2 transcripts using sense (5′-ATGAAGGACAACTTCAGTTTTGCTG-3′) and antisense (5′-AGATGCTTGCCAGGGATTCCTTCT-3′) primers and an annealing temperature = 53° C.

To distinguish between wild type and mutated AT_1 genes, RT-PCR reactions, using Titan One Tube RT-PCR System (Roche), included total RNA, primers which recognized AT_1 but are located outside the neo cassette and thus are common to both wild type and mutated genes (sense: 5′-ATGGCCCTTAACTCTTCTACTG-3′ and antisense: 5′-TGGTTATGGGCATGGCAGTGTCC-3′), [Primer] = 0.4 μ*M*, annealing temperature = 57° C, and cycles = 35.

Controls with heat-inactivated reverse transcriptase or without an RNA template demonstrated that the RNA preparation lacked detectable genomic DNA and that the amplification reaction was without contaminating RNA, respectively.

Fluorescence imaging microscopy. PCT cells were grown to confluence on collagen-coated 12-mm culture plate inserts or on collagen-coated four-well Lab-Tek Chamber Glass Slides (Nalge Nunc International, Naperville, IL), fixed with 4% paraformaldehyde (PFA, Electron Microscopy Sciences, Ft. Washington, PA) in Dulbecco's phosphate-buffered saline (DPBS, Life Technologies, Inc./GibcoBRL) for 30 min. PFA was removed by three brief DPBS washes and monolayers were subsequently treated with quenching buffer (75 m*M* NH_4Cl and 20 m*M* glycine prepared in DPBS) for 10 min to stop fixation, washed three times with DPBS for 5 min, and permeabilized with 0.1% Triton X-100 and 0.05% Saponin (Sigma-Aldrich) in blocking buffer (5% donkey, 5% goat serum, 1% bovine serum albumin, and 5% FBS in DPBS) for 10 min. To specifically stain the apical membrane surface, 100 μg Texas Red–labeled wheat germ agglutinin (WGA-TR; Molecular Probes, Inc.), prepared in DPBS, and was added to the apical monolayer surface for 30 min at room temperature before permeablization. WGA-TR was removed by three 5-min DPBS washes and subsequently postfixed for 10 min with 4% PFA. To confirm confluency by demarking lateral cell borders at the tight junction and confirm cell polarization, cells were treated for 0.5 h at 4° C, with 1:500 dilution 0.5 μg/ml anti-ZO-1 (Zymed Laboratories, Inc., San Francisco, CA), or with 20 μg/ml anti-acetylated tubulin (Clone 6-11B-1 C; Sigma-Aldrich), respectively. Anti-ZO-1 and anti-acetylated tubulin were detected with Alexa 595-labeled secondary antibody (1:1000 dilution; Molecular Probes, Inc.), incubated for 60 min at room temperature. Following antibody incubation and, if necessary, post fixation, monolayers were rinsed three times with DPBS for 5 min and dried for 1 to 3 min. Then, the cell-containing membrane was carefully removed from the insert, placed on a glass slide, and treated with 75 μl VECTASHIELD® or VECTASHIELD® + DAPI (Vector Laboratories, Inc., Burlingame, CA), according to the manufacturer's directions. A #1.5 glass coverslip, which was elevated by spacers to preserve cell height and morphology, was placed on top of the preparation.

Image stacks were acquired with an Inverted Zeiss 200M Microscope (×63, 1.4 NA oil immersion lens) with a Sutter DG4 fluorescent light source and a CoolSnapHQ camera (12 bit depth; Roper Scientific, Inc., Trenton, NJ) under the control of Metamorph v. 4.5 (Molecular Devices, Sunnyvale, CA). Images were deconvolved by AutoQuant's Autodeblur (blind deconvolution) software (AutoQuant Imaging Inc., Troy, NY).

Electrical conductance and electrophysiology. Detailed electrophysiology and electrical conductance measurements were conducted as previously described (Romero et al., 1992; Woost et al., 1996). PCT cells were grown to confluence on 12-mm collagen-coated culture plate inserts in EM at 33° C. In some experiments cells were shifted to DM for 24 to 48 h at 39° C prior to electrophysiology. Inserts were mounted in a modified Ussing chamber equipped with a conventional four-electrode system for measuring transepithelial potential, conductance (G), and short circuit current (Isc). Apical and basal compartments were perfused continuously, simultaneously, and symmetrically with a modified Ringer's solution composed of 100 m*M* NaCl, 4.7 m*M* KCl, 2.4 m*M* $CaCl_2$, 1.2 m*M* $MgCl_2$, 7 m*M* *N*-methyl-D-glucamine, 5 m*M* D-glucose, 2.4 m*M* L-glutamine, 10 m*M* HEPES, and 28 m*M* $NaHCO_3$, pH 7.5. To measure phosphate and succinate transport, the apical perfusate was acutely supplemented with 2 m*M* sodium succinate, pH 7.5, or 1 m*M* sodium phosphate, pH 7.5, respectively, and the change in Isc was measured. Experiments were usually conducted in voltage-clamp mode. Some experiments, however, were conducted in current-clamp mode, and Isc was calculated using Ohm's law. If cells were maintained—immediately prior to electrophysiology—at 33° C or at 39° C for 24 to 48 h, then experiments were conducted at 33° or 37° C, respectively. Measurements are reported as the average ± standard deviation, and "n" represents the number of samples.

Immunoblot analysis of AT_1. Wild type and (AT_{1A} [−/−], AT_{1B} [−/−]) proximal tubule cells were grown to confluence on 12-mm culture plate inserts. Culture media were removed, cells were washed three times with HBSS, and filters containing cells were cut from the surrounding plastic collar and placed in 50 μl 2× Laemmli sample buffer. Proteins from equal sample volumes (typically, 20 μl) of wild type and (AT_{1A} [−/−], AT_{1B} [−/−]) cell lysates were resolved on 10% polyacrylamide-SDS gels (0.75 mm) under reducing conditions, and then transferred to Immobolin-P^{SQ} Transfer Membranes (Millipore Corp.). A standard immunoblot procedure was used, which included a wash buffer composed of 20 m*M* Tris, pH 7.6; 137 mmol/L NaCl, 0.1%; Tween 20 (TBST); and a blocking and antibody binding buffer composed of TBST plus

10% nonfat dry milk. Primary antibodies were AT_1 (N-10) HRP conjugate (a rabbit polyclonal antibody raised against a peptide mapping within the N-terminal extracellular domain of human AT_1, which is identical to the corresponding rat sequence; 1:15,000; Santa Cruz Biotechnology, Santa Cruz, CA), AT_1 (306) (a rabbit polyclonal antibody raised against a peptide corresponding to amino acids 306–359 of human AT_1; 1:200; Santa Cruz Biotechnology), and AT_1 (4H2) (a mouse monoclonal antibody raised against amino acids 229–246 of the third intracellular loop of human AT_1; 1:8,000; Frei et al., 2001). Secondary antibodies were donkey anti-rabbit IgG-HRP conjugate (1:12,500; GE Healthcare Bio-Sciences Corp., Piscataway, NJ) and goat anti-mouse IgG-HRP (1:15,000; EMD Biosciences, San Diego, CA). Detection was accomplished with ECL Plus Western Blotting Detection System (GE Healthcare Bio-Sciences Corp.) and densitometry was performed with VersaDoc Imaging System 3000 using Quantity One 1-D Analysis Software (Bio-Rad Laboratories, Inc., Hercules, CA).

Ang II–mediated β-arrestin 2 translocation. Wild type and combined AT_{1A}/AT_{1B} mutant cells were transfected with β-arrestin 2-p(S65T)GFP (graciously provided by Marc G. Caron, Duke University Medical Center, Durham, NC), using Human Keratinocyte Nucleofector Kit (Amaxa Inc., Gaithersburg, MD) and electroporation program T-18 according to the manufacturer's directions. Transfected cells were seeded onto 35-mm Ethicon collagen-coated Glass Bottom Microwell Dishes (Part No. P35G-1.5-14-C; MatTek Corporation, Ashland, MA), placed in a 33° C incubator, and used 2–5 d later. Prior to agonist stimulation, cells were incubated in serum-free DME-F12 (without any additional additives) for a minimum of 2 h at 33° C, and later, immediately before microscopy, cells were washed with and then maintained in Hank's Balanced Salt Solution (without phenol red). Fluorescence was monitored with an Inverted Zeiss Axiovert 200M Microscope equipped with a Lambda DG-4 Xenon arc lamp, Photometrics Coolsnap HQ digital camera (12 bit depth), CO_2 atmospheric chamber, and heated stage under the control of MetaMorph v. 6.3 (Molecular Devices). Cells were observed with a ×63 1.4 NA oil immersion lens in a 5% CO_2 atmosphere at 33° C. Images were collected at the rate of 1 image per min to yield a time series image stack. After a brief baseline period, cells were stimulated with 10 n*M* [Sar^1]-angiotensin II (Bachem Bioscience Inc., King of Prussia, PA) or combined 1 μ*M* fenoldopam (graciously provided by Neurex Corporation, Menlo Park, CA) and 1 μ*M* isoproterenol (Sigma-Aldrich).

Following image acquisition, cells from image stacks were isolated by cropping with AutoQuant's AutoVisualize + AutoDeblur v. 9.3 (AutoQuant Imaging Inc., Troy, NY) and then processed with MetaMorph Offline v. 4.6r9, using the following algorithm: (1) background subtraction; (2) edge detection using Sobel filter; (3) threshold determination; (4) stack binarization, yielding a combined intracellular vesicle (IV)—plasma membrane (PM) mask; (5) application of the mask to the background-subtracted stack; (6) in some cases, threshold adjustment to minimize the contribution of the PM in order to highlight the IV contribution; and (7) measurement of the total intensity value (TIV) associated with the IV-PM mask. In a similar way the total fluorescence of the cell was determined, but without edge detection. The fractional intensity, i.e., $(TIV)_{IV\text{-}PM}/(TIV)_{Cell}$, was calculated and expressed as a function of time.

To determine the fold change, images 5 or more min before and 3 or more min after agonist treatment were processed separately using the above algorithm. The ratio of the fractional intensities, i.e., $[(TIV)_{IV\text{-}PM}/(TIV)_{Cell}]_{After\ Treatment}/[(TIV)_{IV\text{-}PM}/(TIV)_{Cell}]_{Before\ Treatment}$, yielded the fold change. Statistical comparison was carried out by unpaired, 2-tailed *t*-test. It was applied to the response to angiotensin II in wild type versus mutant cells and in mutant cells to treatment with angiotensin II versus the combination of dopaminergic/adrenergic agonists.

Results

Strategy. This study was undertaken to develop differentiated, conditionally immortalized, transport-competent, Ang-R–deficient cell lines from the S1 segment of the kidney proximal convoluted tubule. Cell lines were *initiated* by breeding Ang-R–deficient mice with an Immortomouse®, genotyping F_2 mice, microdissection and culture of tubule segments, and finally cell outgrowth. Cells from a single tubule outgrowth were passaged as separate isolates. These isolates were *screened* first for monolayer formation and epithelial electrophysiology because these tools are simple and fast, and second, for cell morphology and mRNA expression, which are more time consuming. Separate culture conditions were used for cell *expansion* and *differentiation.* Lastly, cell lines were *characterized* for known indicators of proximal tubule phenotype, including sodium-dependent cotransporters and Ang II–stimulated β-arrestin 2 translocation. Four types of cell lines were established: wild type (32101), AT_{1A} mutant (AT_{1A} [−/−], Tag [+/−]; 0299), AT_{1B} mutant (AT_{1B} [−/−], Tag [+/−]; 53101), and combined AT_{1A}/AT_{1B} mutant (AT_{1A} [−/−], AT_{1B} [−/−], Tag [+/+]; 42601).

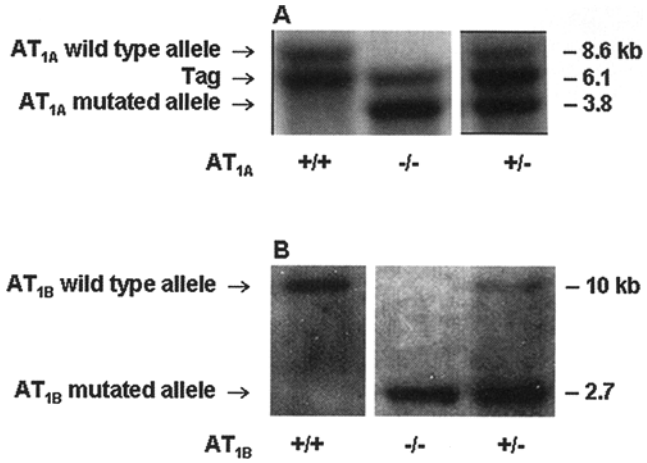

FIG. 1. Southern blot analysis of F_2 mice following breeding of angiotensin receptor–deficient mice with an Immortomouse®. (*A*) Targeted gene: AT_{1A}. An 8.6-kb *Bam*HI fragment identifies the wild type allele, whereas a 3.8-kb *Bam*HI fragment indicates the targeted and mutated allele. The 6.1-kb fragment represents Tag. (*B*) Targeted gene: AT_{1B}. A 10-kb *Hin*dIII fragment identifies the wild type allele, whereas a 2.7-kb *Pst*I/*Hin*dIII fragment indicates the targeted and mutated allele.

Cell line initiation: breeding and genotyping. Breeding a male Immortomouse® with several female Ang-R–deficient mice, i.e., AT_{1A} (−/−) or combined (AT_{1A} [−/−], AT_{1B} [−/−]), successfully produced F_2 progeny that were homo- or heterozygous for Tag as well as homozygous for a targeted and disrupted Ang-R. Mice that were heterozygous for Tag were preferentially sought, because we reasoned that the transformation potential of cells derived from these mice would be less than those from Tag homozygous mice. Genotyping was accomplished by Southern hybridization, and representative blots are shown in Fig. 1. A single mouse sufficed to establish approximately 12 proximal tubule isolates. Cell outgrowth from this material was abundant, and several cultures of each genotype were selected for amplification and long-term culture.

Expansion and differentiation. PCT cells were consistently grown on culture plate inserts to ensure a sufficiently high oxygen flux for the oxidative metabolism needs of the cells while maintaining at the same time a high volume of culture medium to cells to satisfy nutritional needs. Oxygen flux by diffusion through aqueous fluid layers is generally slow because of the limited solubility of oxygen. Therefore, the fluid layer above cells needs to kept below 0.34 mm for mammalian cells to maintain oxidative metabolism in cultures in the absence of mechanical mixing of the medium (Dickman and Mandel, 1989; Wolff et al., 1993; Nowak and Schnellmann, 1995; Allen et al., 2001). We have previously shown that the use of these inserts or a similar product promotes and maintains a differentiated proximal tubule phenotype more effectively than growth on plastic

TABLE 1

PCT SCREENING ASSAY: CELL MONOLAYER ELECTROPHYSIOLOGY AND IMAGING MICROSCOPY

Ang-R status	Basal Isc ($\mu A/cm^2$)	Basal G (mS/cm^2)	2mM Succinate (ΔIsc, $\mu A/cm^2$)	1 mM PO_4 (ΔIsc, $\mu A/cm^2$)	WGA-TR[a]
AT_{1A} −/−	3 ± 1 (3)	10 ± 1 (3)	9 ± 5 (34)	2 ± 1 (3)	+++
AT_{1B} −/−	−3 ± 3 (4)	8 ± 3 (4)	2 ± 2 (4)	3 ± 2 (4)	++++
AT_{1A} −/− AT_{1B} −/−	−2 ± 7 (3)	4 ± 1 (3)	3 ± 1 (3)	2 ± 1 (3)	+++
Wild type	−2 ± 1 (4)	7 ± 2 (4)	2 ± 1 (4)	2 ± 1 (3)	+++

[a] WGA-TR staining, images were compared and scored visually, according to the following scale: ++++, intense and uniform staining, representing densely packed microvilli and a well-defined brush border; +++, less intense, but uniform, staining compared with ++++; +, limited and disperse staining, representing sparse microvilli and a poorly defined brush border, as observed in mCT/CD cells. Measurements are reported as the average ± standard deviation and "n" represents the number of samples.

(Orosz et al., 2004). Under these conditions, cells grow well with just 5 m*M* glucose as major carbon source and do not produce noticeable acidification of the medium within 2 d of media change, as judged by phenol red.

Figure 3*A* shows a ×20 phase contrast image of wild type cells grown to confluence and then fixed. Cells possessed a characteristic, uniform, cobblestone-shaped appearance typical of these and other proximal tubule cells in culture. Other wild type and Ang-R–deficient cell lines exhibited a similar morphologic appearance.

PCT cells were maintained in EM at 33° C. EM is designed to promote cell growth and division and is commonly used for proximal tubule cell cultures. To assess the differentiation potential, cells were grown to confluence and then shifted to DM at 39° C. These conditions were designed to diminish growth stimulation and the influence of the oncogene Tag, as well as eliminate large amounts of albumin and other macromolecules from the apical side. DM is similar to EM, but lacks added growth factors EGF, insulin, and interferon-γ on the basal side, and insulin, interferon-γ, and serum on the apical side. As SV40 large Tag expression is driven by interferon-γ–response elements, omission of this cytokine from the medium decreases Tag expression. In addition, the higher temperature of 39° C promotes inactivation of existing Tag because the mutation used for the Immortomouse® is temperature-sensitive. Omission of serum proteins from the apical side is important because proximal cells actively endocytose apical proteins and overloading of this machinery is thought to be associated with pathological changes in cell phenotype (Erkan et al., 2005).

Cell line screening. All isolates were screened for formation of epithelial monolayers with "cobblestone" appearance. Nearly all microdissected tubules grew out epithelial cells that on passage formed confluent monolayers, regardless of the genotype with respect to Ang-R. This epithelial monolayer organization extended to an area of at least 4.2 cm^2 (i.e., the effective membrane area of a 30-mm-diameter culture plate insert). To quantify overall monolayer properties, the transepithelial conductances (G) was measured under sterile conditions. The values of the selected cell lines ranged from 2 to 10 mS/cm^2 (Table 1). These values are lower than ones measured in intact tubules of about 100 to 150 mS/cm^2 (Lutz et al., 1973; Baum and Quigley, 2005), i.e., the specific resistance (inverse of conductance) of the cell lines is actually higher than tubules. The measured resistance values indicate formation of tight junctions between cells. The rationale for selecting cell lines with these values is that (1) monolayer resistance value can be artificially lowered by defects in the monolayer, and (2) higher resistance monolayers facilitate functional quantification of cotransporter expression, such as Na_3^+–succinate and Na_3^+–phosphate co-transport.

Screening: confirmation of genotype by mRNA expression. Figure 2*A* shows RT-PCR analysis of AT_{1A} and AT_{1B} transcripts in wild type and mutant cell lines as well as *Eco*R1 digestion of the amplification products. The primers were expected to yield a 305-bp product for both AT_{1A} and AT_{1B}. The two AT_1 receptor subtypes can be distinguished on further *Eco*R1 digestion because AT_{1A} yields fragments of 128 and 177 bp while AT_{1B} is resistant to *Eco*R1. As predicted, wild type cells contained both digested AT_{1A} and resistant AT_{1B} products; AT_{1A} (−/−) cells contained only the resistant AT_{1B} product; and AT_{1B} (−/−) cells contained only the digested AT_{1A} product. The combined (AT_{1A} [−/−], AT_{1B} [−/−]) cells contained neither product. The integrity of the mRNA isolated from the combined AT_{1A}/AT_{1B} mutant was confirmed, by incubating it with primers directed against AT_2 and observation of the expected 480-bp product (data not shown). Thus, mRNA expression in each of the cell lines coincided with the designated genotype.

These results were confirmed by an additional experiment using primers located within the AT_1 coding sequence but outside the region of the gene disrupted by insertion of the neo cassette. PCR products of approximately 900 and 1600 bp are diagnostic of wild type and mutated AT_{1A}/AT_{1B}, respectively (Fig. 2*B*).

Screening: morphology and immunocytochemistry. In vivo, the apical surface of the proximal tubule is characterized by a prominent, well-developed brush border (Kriz and Knissling, 1992), composed of slender, tightly packed, uniform-shaped microvilli, containing on its surface many highly glycosolated proteins. Wheat germ agglutinin (MW 36,000) is a lectin that preferentially binds to membrane glycoproteins, specifically dimers and trimers of *N*-acetylglucosamine (Scherberich et al., 1977), and this characteristic has been exploited in the isolation and purification of proximal tubule brush border membrane vesicles (Marshansky et al., 1997).

In PCT cell lines the density and uniformity of the brush border were assessed by fluorescence imaging microscopy of WGA-TR binding. Cells were scored by visual comparison with other cell lines, including conditionally immortalized mouse connecting tubule or collecting duct (mCT/CD) cells. In contrast to PCT cells, mCT/CD cells have short, stubby, less prominent microvilli and a poorly defined brush border (Kriz and Knissling, 1992). Without exception, cells having the functional transport properties of PCT cells as determined by electrophysiology (Table 1 and Fig. 4) were scored at 4+s or 3+s. However, cells, which were functionally more similar to mCT/CD cells in terms on amiloride-sensitive potentials

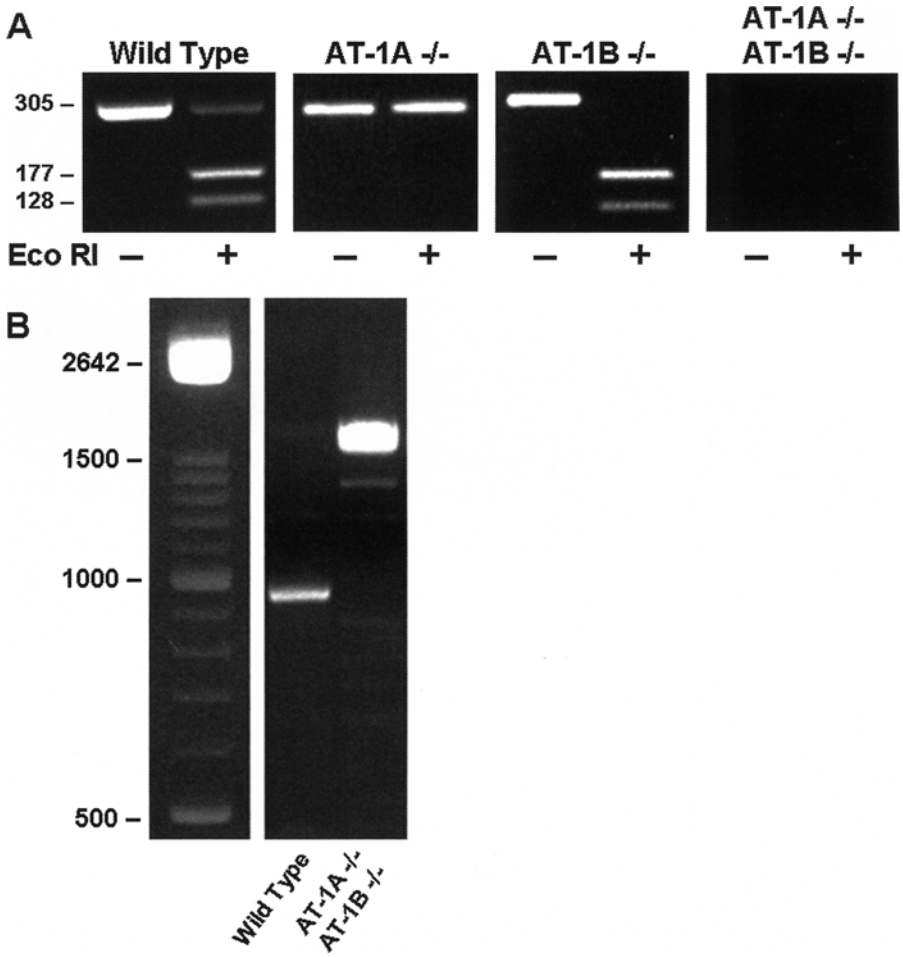

FIG. 2. Angiotensin receptor transcripts in wild type and mutant cell lines. (*A*) mRNA was isolated, analyzed by RT-PCR, and the amplification products were treated with (+) or without (−) 20 units *Eco*R1, as described in Materials and Methods. The sense primer is common to wild type AT_{1A} and AT_{1B}, but not the mutated genes, whereas the antisense primer is common to both wild type and mutant AT_{1A} and AT_{1B}. *Eco*R1 digestion of the 305-bp AT_{1A} product yields fragments of 128 and 177 bp, whereas the AT_{1B} product is resistant to digestion. mRNA expression coincides with the genotype of each cell line. (*B*) Total RNA from wild type and (AT_{1A} [−/−], AT_{1B} [−/−]) cells was probed with primers which recognize AT1 sequences outside the region disrupted by the neomycin (neo) cassette. The 900-bp product is diagnostic of wild type AT1, whereas the larger product (approximately 1600 bp) is characteristic of mutated AT1. The *left lane* is a 100-bp DNA ladder.

(see below), stained much less intensely and were evaluated as 1+. See Table 1 and Fig. 3*B*.

Tight junctions or zonula occludens of renal proximal tubule cells separate the tubule lumen from the basolateral intercellular space, define the boundary between the apical and basolateral plasma membranes, restrict protein and lipid diffusion between membrane domains, and serve as selective permeability barriers for solute and water transport (Alberts et al., 2002). A number of proteins are associated specifically with tight junctions, including ZO-1, which is thought to interact with other junctional proteins and the actin cytoskeleton. Figure 3*C* shows ZO-1 staining of wild type cells. ZO-1 is uniformly distributed at the cell periphery, along points of cell–cell contact. Such staining is characteristic of epithelial cells, including PCT cells. All cell lines showed similar patterns of ZO-1 staining.

The primary cilium is a solitary structure arising from the supranuclear centriole and is reasoned to be a flow sensor converting mechanical cues to chemical signals (Praetorius and Spring, 2001), opening Ca^{2+}–sensitive intermediate-conductance K^+ channels (Praetorius et al., 2003). Primary cilia, as detected by an antibody against acetylated tubulin, were abundant in confluent PCT cells in differentiation medium. In the field of cells shown in Fig. 3*D*, primary cilia were observed on 11 of 15 cells. Under the same differentiation conditions, all cell lines exhibited similar, abundant cilia.

Characterization: electrolyte transport. To assess functional expression of proximal tubule cotransporters, changes in short-circuit current (ΔIsc) of confluent monolayers were measured between basal state and following apical addition of cotransporter substrate. The basal transepithelial short-circuit current (Isc) ranged from approximately −3 to 3 μA/cm² (Table 1). In two of the five reported cell lines, Isc was slightly positive, representing net anion secretion (or cation absorption) and thus a slightly lumen negative potential under open circuit conditions (Table 1). In contrast, the Isc of the three remaining cell lines was slightly negative, representing net cation secretion (or anion absorption) and thus a slightly lumen positive potential under open circuit conditions (Table 1). These properties are in reasonable agreement with the electrical properties of primary cultures of human proximal tubule cells measured by Todd et al. (1993). In that study, conductances and short-circuit currents ranged from 0.8 to 5 mS/cm² and from −2 to +7 μA/cm², respectively.

Apical succinate uptake is mediated by the renal low affinity Na^+/dicarboxylate cotransporter (Slc13a2 or NaDC-1). Transport is electrogenic with a stoichiometry of 3 Na^+ ions to 1 dicarboxylate ion. The K_m for succinate is approximately 0.5 m*M* (Pajor, 2000).

As shown in Fig. 4*A*, when the apical perfusate of cells was supplemented with 2 m*M* succinate, the Isc increased from approximately 2 to 6 μA/cm² (or ΔIsc is approximately 4 μA/cm²). In other cell lines, ΔIsc ranged from approximately 1 to 9 μA/cm² following succinate addition (Table 1). The positive values of ΔIsc were con-

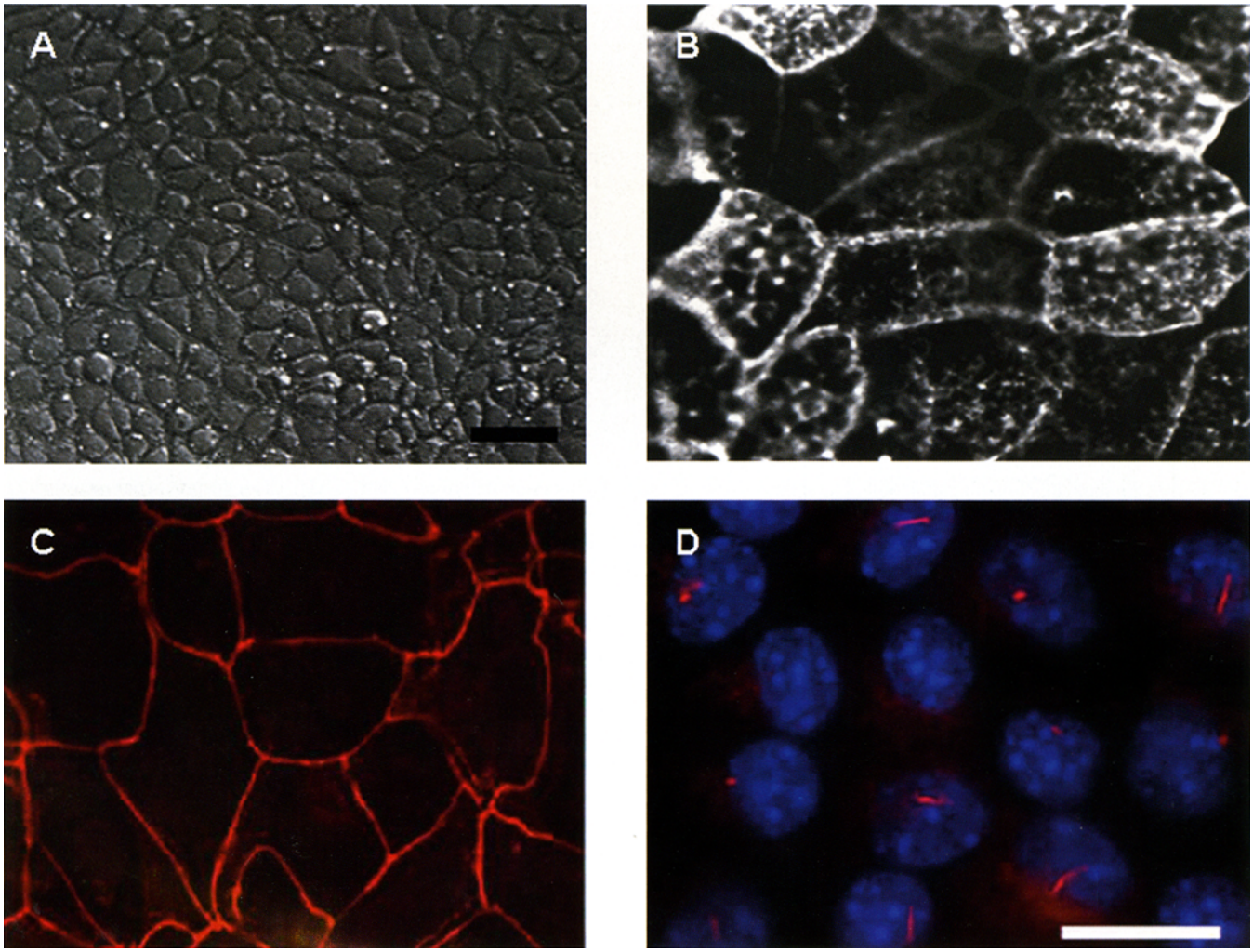

FIG. 3. Immunocytochemistry. (*A*) ×20 phase contrast image of wild type cell monolayer on a collagen-coated chamber glass slide. *Note* the uniform, "cobblestone" appearance of the monolayer. (*Calibration bar* = 20 μm) (*B*) ×100 epifluorescence image of confluent wild type monolayer showing the apical surface stained with Texas Red–labeled wheat germ agglutinin. The brush border is uniformly and robustly defined over the entire apical surface with more intense staining near the cell periphery. (*C*) ×63 subapical, supranuclear, confocal slice of confluent wild type monolayer stained with an antibody against ZO-1. Cell boundaries, cell–cell contact, and tight junctions are clearly delineated. (*D*) ×63 epifluorescence color combined image of confluent wild type monolayer stained with an antibody against acetylated tubulin to illuminate cilia and with DAPI to visualize nuclei. Primary cilia are observed on 11 of 15 cells. (*Calibration bar* = 10 μm) The morphologic features shown in images *A* through *D* are representative of all cell lines.

sistent with the transit of positively charged ions from the apical to the basal compartments and electrogenic succinate reabsorption. Similar results were observed with other PCT cell isolates.

Similarly, proximal tubular phosphate recovery is mediated by the Na_3^+–phosphate cotransporter (Slc34a1 or Na-P_i cotransporter [type IIa]). This cotransporter is electrogenic and mediates the transit of 3 Na^+ ions to 1 HPO_4^{-2} ion with a K_m for phosphate of 0.1 to 0.2 m*M* (Murer et al., 2000).

When the apical perfusate of cells was supplemented with 1 m*M* phosphate, the ΔIsc was approximately 1 to 3 μA/cm² (Table 1 and Fig. 4*B*). These results were consistent with the net movement of positively charged ions from the apical to basal compartments and electrogenic transport of Na^+ and phosphate. Similar results were observed with other PCT cell isolates. Both succinate and phosphate transport was detectable after cells became confluent at the permissive temperature of 33° C and was not changed by incubation in DM for 24 h at 39° C. This response to temperature (differentiation conditions) differed from the appearance of primary cilia, which were much more pronounced after monolayers had been moved to 39° C.

During the screening process, a few cortical cell lines exhibited basal Isc's that ranged from approximately 25 to 40 μA/cm² of net cation absorption (anion secretion). These relatively high basal Isc's were completely inhibited by the apical addition of 10 μ*M* amiloride, a sodium channel inhibitor. Furthermore, neither phosphate nor succinate was transported by these cells (ΔIsc = 0, following addition of 1 m*M* phosphate or 2 m*M* succinate). We concluded that these cell lines have a phenotype consistent with cortical, late distal tubules and that we could easily distinguish between cells derived from the proximal or distal tubule. No cultures with intermediate

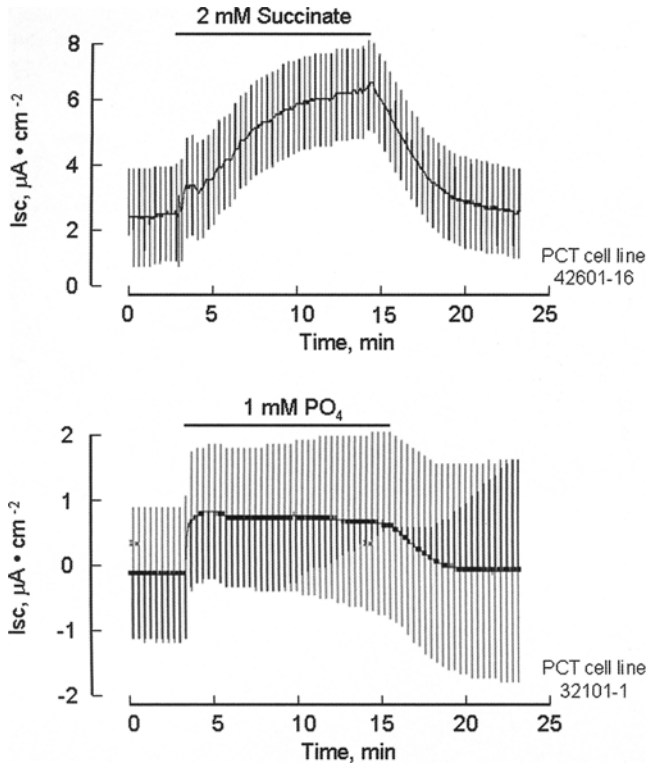

FIG. 4. Succinate- and phosphate-stimulated short-circuit current (Isc) in mPCT cells. Transepithelial Isc was measured in a confluent monolayer of PCT 42601 or 32101 cells, as described in Methods. Apical and basal compartments were perfused independently with a modified Ringer's solution. Acute apical addition of 2 m*M* Na_2succinate or 1 m*M* Na_2HPO_4 increased Isc, which corresponds to movement of net positive charge from the apical to the basal side of the monolayer and is consistent with increased Na^+ absorption. These experiments are representative of the succinate and phosphate experiments summarized in Table 1.

properties were observed, consistent with derivation of cell lines from single, microdissected tubules.

Characterization: immunoblotting of AT_1 in wild type and (AT_{1A} [−/−], AT_{1B} [−/−]) cells. The animal models, from which the cell lines were derived, had been characterized in terms of receptor function and binding of physiological Ang II concentrations and are clearly functional "knock-outs" (Ito et al., 1995). To assess the presence of protein, immunoblotting was carried out with three different antibodies, each recognizing a distinct region within Ang-R, one close to the N-terminus, another close to the C-terminus and the third towards the third intracellular loop. The specificity of these antibodies had previously been established in other cell systems (Frei et al., 2001). Equal amounts of lysates from wild type and (AT_{1A} [−/−], AT_{1B} [−/−]) cells were analyzed for immunoreactive AT_1. The immunoblot analysis (Fig. 5) showed that each antibody recognized a 41-kDa protein in both cell types. AT_1 (306) antibody recognized approximately equal levels of the 41-kDa protein. However, both AT_1 (N-10) and (4H2) antibodies detected more immunoreactive protein in mutant compared with wild type cells. Densitometry of these protein bands indicated that the ratios of detected immunoreactive AT_1 for mutant to wild type cells are 1.1 and 1.8 for anti-AT_1 (N-10) and anti-AT_1 (4H2), respectively. In addition, AT_1 (306) recognized a second larger protein at 74 kDa, presumably a homo- or hetero-oligomer of AT_1. Thus, despite experiments which show that (AT_{1A} [−/−], AT_{1B} [−/−]) cells possess the designated genotype (Fig. 1) and expected transcript expression (Fig. 2*A* and *B*), these mutant cells express a 41-kDa species recognized by several different antibodies against AT1. These data suggest that either the modified AT1a(−) or AT1b(−) gene or both give rise to a protein with similar antigenic properties and molecular weight as the native one at the N-terminus and from the third intracellular loop to the C-terminus, but must differ in the region between the N-terminus and the third intracellular loop.

Characterization: Ang II–mediated β-arrestin 2 translocation in wild type and (AT_{1A} [−/−], AT_{1B} [−/−]) cells. To assess the functionality of the Ang-R in wild type and mutant cells, Ang II–mediated β-arrestin 2 translocation was measured. In addition to the classical paradigm of GPCR-mediated second messenger generation, agonist activation of 7TMRs also directs, in a G protein–independent fashion, the formation of cytoplasmic signaling complexes via β-arrestins (reviewed by Lefkowitz and Shenoy, 2005). As Caron, Lefkowitz, and others have shown, the translocation of GFP-labeled β-arrestin has been exploited as a measure of 7TMR activation (Barak et al., 1997; Ferguson and Caron, 2004; Shenoy and Lefkowitz, 2005). Therefore, we measured the dynamics of angiotensin-dependent translocation of GFP-β-arrestin 2 by live cell microscopy. Treatment of wild type cells with 10 n*M* angiotensin II

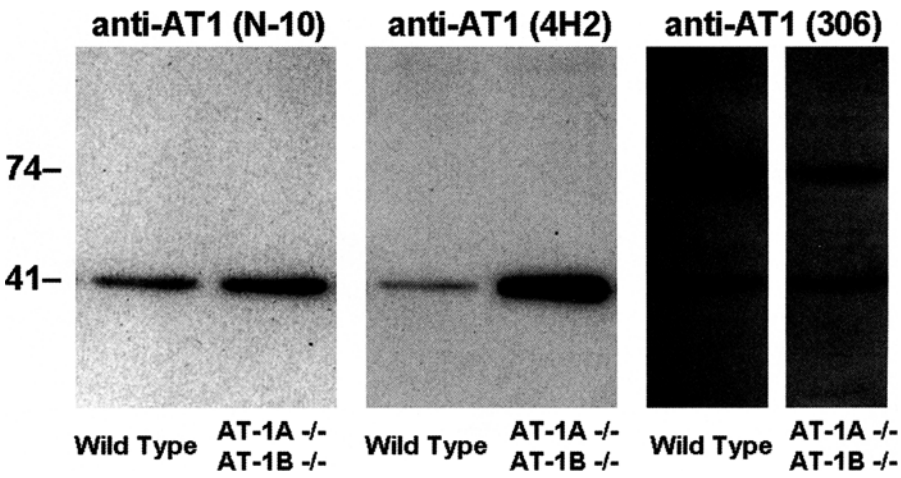

FIG. 5. Immunoblot analysis of AT_1 in wild type and [AT_{1A} (−/−), AT_{1B} (−/−)] mPCT cells. Filters containing confluent cell cultures were washed, cut from the surrounding plastic collar, and placed in Laemmli sample buffer. Equal sample volumes were resolved on a 10% polyacrylamide-SDS gels, transferred to a PVDF membrane, and probed with anti-AT1 (N-10) HRP conjugate, anti-AT1 (4H2), and anti-AT1 (306). Visualization was accomplished with an appropriate secondary antibody, if required, and chemiluminescence detection.

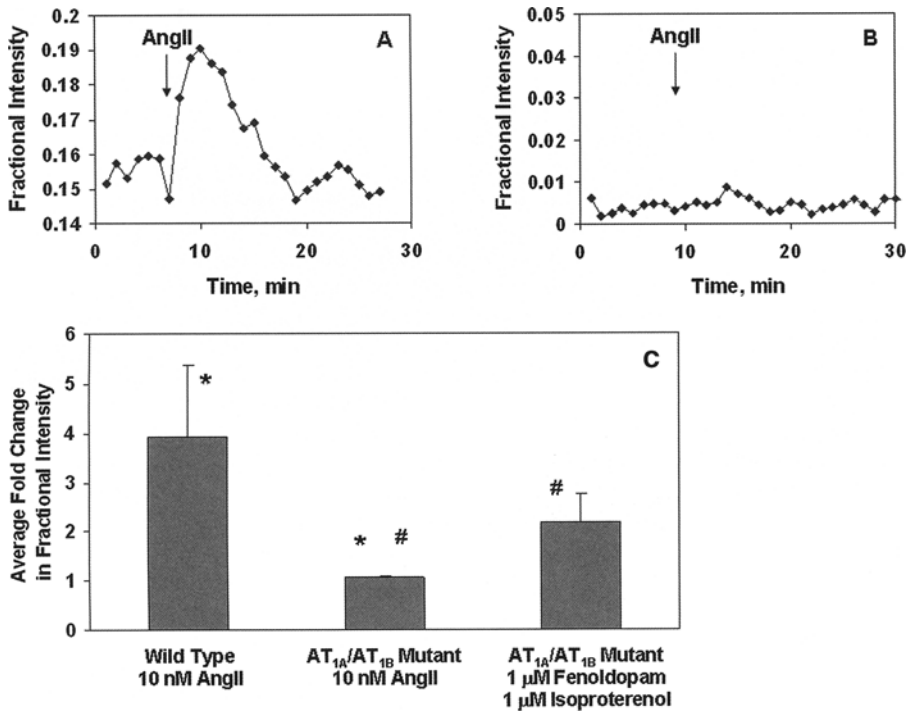

FIG. 6. Angiotensin II (Ang II)–mediated β-arrestin translocation in wild type and [AT_{1A} (−/−), AT_{1B} (−/−)] mPCT cells. Cells were transfected with β-arrestin 2-GFP, treated with 10 n*M* [Sar^1]-angiotensin II or combined 1 μ*M* fenoldopam and 1 μ*M* isoproterenol, and fluorescence was monitored and analyzed as described in Methods. (*A*) Ang II–stimulated fluorescence increase in 1 wild type cell. (*B*) Ang II treatment of 1 AT_{1A}/AT_{1B} mutant cell. (*C*) Data summary showing 10 n*M* angiotensin II treatment of wild type (n = 3) and AT_{1A}/AT_{1B} mutant (n = 3) cells as well as combined 1 μ*M* fenoldopam and 1 μ*M* isoproterenol-stimulated β-arrestin translocation in AT_{1A}/AT_{1B} mutant (n = 7) cells. Data are expressed as the mean ± standard deviation; *, # $P < 0.05$.

stimulates an increase in the ratio of β-arrestin 2 fluorescence associated primarily with the fluorescence of intracellular vesicles (IV) (with some contributions from the fluorescence associated with the plasma membrane; Fig. 6*A* and *C*). This increase is associated mainly with an increase in the number and fluorescence intensity of endocytic vesicles, and represents internalization of the angiotensin receptor-β-arrestin 2 complex. Results were normalized between experiments by calculating the ratio, i.e., fractional intensity, between the fluorescence associated with IV-PM and the total cellular fluorescence. In contrast, the fluorescence intensity remained unchanged when (AT_{1A} [−/−], AT_{1B} [−/−]) cells were treated with Ang II (Fig. 6*B* and *C*), suggesting the inability to detect functional AT_{1A} and AT_{1B} receptors in these double mutant cells. Yet, combined treatment with 1 μ*M* fenoldopam and 1 μ*M* isoproterenol demonstrated, however, that (AT_{1A} [−/−], AT_{1B} [−/−]) cells contain a functional β-arrestin 2–mediated system of endocytosis (Fig. 6*C*). Thus, this assay suggests that wild type and (AT_{1A} [−/−], AT_{1B} [−/−]) cells are functionally distinct with respect to angiotensin II–mediated receptor activation.

DISCUSSION

In cell culture, differentiated somatic cells have a limited life span: cells divide a finite number of times, arrest (a process called senescence), and eventually undergo cell death, which is related to telomerase repression and telomere shortening. By introducing specific viral oncogenes or inducing telomerase activity, cellular programs for limiting the rate and number of cell replications are inhibited, and immortalization is initiated. Three primary methods have emerged to overcome senescence and crisis, to initiate cellular immortalization, and to develop specific cell lines: (1) introduction of viral oncogenes by either transfection or viral-mediated gene transfer into primary or early passage cultures, (2) creation of transgenic animals harboring a regulated immortalizing gene, which is not functionally active under in vivo conditions, but can be activated in vitro, and (3) induction of telomerase activity to increase the proliferative potential of cultured cells (Hopfer et al., 1996; Yeager and Reddel, 1999). Strategies 1 and 3 are suitable for the development of many types of mammalian cell lines, including cells of human origin. Strategy 2 has resulted in the development of the Immortomouse®, which harbors a temperature-sensitive mutation of SV40 large Tag. Expression of this mutation can be turned off in cell culture to study differentiation or after cell transplantation to a host animal, such as a nude mouse. Further, this methodology can be extended by breeding an Immortomouse® with any transgenic or gene-targeted mice to generate corresponding conditionally immortalized cell lines.

Following establishment of low passage number cultures, cell lines are screened and then selected according to various predetermined criteria, including those differentiated functions or markers that are important for the objectives of the proposed study. For the development of transporting epithelia, such as the PCT cells reported here, these criteria include polarized orientation, tight junction formation, characteristic cell surface markers, and functional electrolyte transport. Cell lines that retain the phenotypic properties of the originating tissue are subsequently amplified and cryopreserved.

Despite its important immortalizing effects, Tag expression in cultured cells is also potentially problematic. The effects of Tag on the cell cycle and cellular differentiation are complex, remain incompletely understood, and in some cases may result in genomic instability (Hopfer et al., 1996). A major advantage of this approach, which develops matched sets of cell lines from gene-targeted mice, is insertion of the immortalizing transgene into the same chromosomal location in all cell lines, and hence any unintended, Tag-

induced effects should be similar among all cell lines. Alteration of the cellular phenotype, should it occur, may be related to a specific cell type, level of Tag expression, or the cumulative duration of Tag-harboring cells in culture. Loss of phenotype is usually overcome by reverting to an earlier passage of the same cell line. Examples of established cell lines derived from the Immortomouse® include glia, bone marrow stroma, osteoclast precursors, primitive kidney cells, astrocytes, and skeletal myoblasts (reviewed in Hopfer et al., 1996).

We detail here the successful development of an entire set of conditionally immortalized, transport competent, Ang-R–deficient cell lines from the S1 segment of the PCT. These include AT_{1A} (−/−), AT_{1B} (−/−), combined (AT_{1A} [−/−], AT_{1B} [−/−]), and wild type cell lines. Importantly, all cells grow well in culture and have the potential to differentiate to a proximal tubule phenotype under appropriate conditions, indicating that AT_1 receptors are not essential for cell growth and differentiation. However, a requirement for the presence of at least one type of Ang-R for cell growth and differentiation cannot be excluded, because generation of cell lines lacking combined $AT_{1A}/AT_{1B}/AT_2$ receptor subtypes was not attempted.

The state of differentiation that cells achieve in culture is subject to both cell line origin, history, and culture conditions. We derived these cell lines by microdissection of tubules that clearly identified their origin. This combination of Immortomouse® and microdissection has the advantage that cell line establishment is by a process that resembles wound healing and favors retention of differentiated features. In contrast, immortalization by transfection in vitro requires cloning of cells with loss of differentiated features in many cells due to forced growth without neighboring epithelial cells, at least for some time. Consequently, cell line isolation by the Immortomouse®–microdissection method involves less of a selection bias compared to common in vitro transfection methods. The robustness of the Immortomouse®–microdissection strategy is expressed by an efficiency of 60 to 80% in converting cultures of microdissected tubules into cell lines and by monolayer properties of separate isolates that are quite similar.

The relevance of cell lines for physiological or pathophysiological studies depends to a large extent on their potential to take on a differentiated phenotype. By definition, cells undergoing division lose their differentiated phenotype. Only after withdrawal from the cell cycle can cells restore a genetic program that leads to differentiation in morphology and function. The observations that nonrenal stem cells can differentiate to proximal tubule cells in vivo, even if that is a rare event (Lin et al., 2003), indicates that important cues for initiating genetic programs of differentiation are provided by the micro-environment. Little is known about these factors which are crucial for redifferentiation of adult cells. However, some useful strategies have been established for obtaining a differentiated phenotype in vitro, which were implemented in this study. These include: (1) promotion of retaining memory of the previously differentiated state by expanding cells on a matrix and at densities so that contact with neighboring epithelial cells can be established and cell spreading is similar to wound healing; (2) conditions favorable for retaining the oxidative metabolism by culturing cells on permeable support with only a thin fluid layer above the cells; (3) decreased growth factor stimulation after termination of the expansion phase (removal of EGF, insulin, and interferon-γ from the basal side and insulin, interferon-γ, and serum from the apical side). While the importance of these considerations has been known for some time, they have not been consistently incorporated into even recent studies. For example, there is considerable interest in the effects of hyperglycemic glucose concentrations on proximal tubule functions due to the increased incidence in diabetes and renal diabetic complications in the population. Unfortunately, the meaning of data can be called into question when the data come from cell studies complicated by simultaneous, uncontrolled hypoxia (Morais et al., 2005; Panchapakesan et al., 2005; and references therein).

Another aspect of cell line generation concerns the stringency of criteria used to judge the differentiation status of cells. It is worthwhile summarizing the ones used in this study: (1) contact inhibition of cells upon confluency and formation of macroscopic, electrically resistive monolayers; (2) polarization of cells, including that of the microtubular cytoskeleton with formation of a primary cilium on the apical surface, which can arise only after the cell's centriole has been converted to the basal body and the mother centriole nucleates the axoneme of the cilium; (3) oxidative metabolism; (4) expression of proximal tubule specific cotransporter functions.

Even at the permissive temperature of 33° C, cells were contact-inhibited upon confluence to some extent and expressed a proximal tubule phenotype in terms of Na_3^+–phosphate and Na_3^+–succinate cotransport. However, other differentiated features of cilium maturation and apical receptor trafficking were observed only after switching to 39° C (Kolb et al., 2004).

Recent work has demonstrated the importance of using cell lines with a defined cellular phenotype and its effect on transport function (Gross et al., 2001). In this study proximal tubule cells were transfected with Na^+–bicarbonate cotransporter clones p-NBC1 (from pancreas) and k-NBC1 (from kidney) and the resulting transport stoichiometry was 3 bicarbonate to 1 Na^+, which is crucial for proximal tubule bicarbonate reabsorption in vivo (Muller-Berger et al., 1997). In contrast, transfection of the same clones into collecting duct cells yielded a stoichiometry of 2 to 1. Thus, the cellular components of the different cell types played a defining role in ion transport and cell homeostasis.

Sets of matched cells lines with few defined differences offer many advantages for detailed in vitro studies, and should, for example, help solve some of the difficult cell biological problems of angiotensin-regulated proximal tubule function. For example, proximal tubule cell lines derived from spontaneously hypertensive and normotensive rats (Woost et al., 1996) have been used extensively to study angiotensin- and dopamine-mediated effects in hypertension (Xu et al., 2000; Yu et al., 2000; Zeng et al., 2003a, 2003b, 2004). Notably, these cell lines accurately mimicked the in vivo differences observed in intact animals and offered the further advantage of modeling the renal hypertensive phenotype at the cellular and molecular levels. In a similar manner, comparative studies between various Ang-R–deficient cell lines as well as transfection of functional receptors into deficient cell lines should provide detailed insights into angiotensin regulation not previously achieved. Potential studies include the relationship between receptor activation and electrolyte reabsorption or receptor trafficking and cell signaling. In addition, this set of Ang-R–deficient cell lines may prove to be an important pharmaceutical tool for the screening and development of Ang-R antagonists to help treat hypertension.

In principle, the technology reported here is applicable to other tissues, cell types, and proteins. It requires the availability of appropriate gene targeted mice and knowledge about appropriate cell culture conditions. In the case of more complex tissues with several

cell types, cell separation methods are also necessary. If fluorescent tags for surface markers are available, then fluorescence activated cell sorting becomes a realistic approach. These cell lines and others developed by similar approaches are, therefore, potentially important and useful models to probe biologically complex questions at the cellular and molecular levels.

Acknowledgments

This work was supported by National Institutes of Health (NIH) grants DK027651, HL-41618, and P30CA43703-12. RJK was supported by NIH grant DK-07678. We acknowledge the technical assistance of Sheryl Chow and her contribution to the immunoblot analysis of AT_1.

References

Alberts, B.; Johnson, A.; Lewis, J.; Raff, M.; Roberts, K.; Walter, P. Molecular biology of the cell: cell junctions, cell adhesion, and the extracellular matrix, 4th ed. New York: Garland Science (Taylor & Francis Group); 2002:1065–1125.

Allen, C. B.; Schneider, K.; White, C. W. Limitations to oxygen diffusion and equilibration in in vitro cell exposure sustems in hyperoxia and hypoxia. Am. J. Physiol. Lung Cell. Mol. Physiol. 281:L1021–L1027; 2001.

Barak, L. S.; Ferguson, S. S. G.; Zhang, J.; Caron, M. G. A β-arrestin/green fluorescent protein biosensor for detecting G protein-coupled receptor activation. J. Biol. Chem. 272:27497–27500; 1997.

Baum, M.; Quigley, R. Maturation of rat proximal tubule chloride permeability. Am. J. Physiol. Regul. Integr. Comp. Physiol. 289:R1659–R1664; 2005.

de Gasparo, M.; Catt, K. J.; Inagami, T.; Wright, J. W.; Unger, T. International union of pharmacology. XXIII. The angiotensin II receptors. Pharmacol. Rev. 52:415–472; 2000.

Dickman, K. G.; Mandel, L. J. Glycolytic and oxidative metabolism in primary renal proximal tubule cultures. Am. J. Physiol. Cell Physiol. 257:C333–C340; 1989.

Dinh, D. T.; Frauman, A. G.; Johnston, C. I.; Fabiani, M. E. Angiotensin receptors: distribution, signalling and function. Clin. Sci. (Lond.) 100:481–492; 2001.

du Cheyron, D.; Chalumeau, C.; Defontaine, N.; Klein, C.; Kellermann, O.; Paillard, M.; Poggioli, J. Angiotensin II stimulates NHE3 activity by exocytic insertion of the transporter: role of PI 3-kinase. Kidney Int. 64:939–949; 2003.

Erkan, E.; Devarajan, P.; Schwartz, G. J. Apoptotic response to albumin overload: proximal vs. distal/collecting tubule cells. Am. J. Nephrol. 25:121–131; 2005.

Ferguson, S. S. G.; Caron, M. G. Green fluorescent protein-tagged β-arrestin translocation as a measure of G protein-coupled receptor activation. In: Smrcka, A. V., ed. Methods in molecular biology: G protein signaling methods and protocols. Totowa, NJ: Humana Press; 2004:121–126.

Frei, N.; Weissenberger, J.; Beck-Sickinger, A. G.; Höfliger, M.; Weis, J.; Imboden, H. Immunocytochemical localization of angiotensin II receptor subtypes and angiotensin II with monoclonal antibodies in the rat adrenal gland. Regul. Pept. 101:149–155; 2001.

Gross, E.; Hawkins, K.; Abuladze, N.; Pushkin, A.; Cotton, C. U.; Hopfer, U.; Kurtz, I. The stoichiometry of the electronic sodium bicarbonate cotransporter NBC1 is cell-type dependent. J. Physiol. 531:597–603; 2001.

Hopfer, U.; Jacobberger, J. W.; Gruenert, D. C.; Eckert, R. L.; Jat, P. S.; Whitsett, J. A. Immortalization of epithelial cells. Am. J. Physiol. 270 (Cell Physiol. 39):C1–C11; 1996.

Ichiki, T.; Labosky, P. A.; Shiota, C., et al. Effects on blood pressure and exploratory behavior of mice lacking angiotensin II type-2 receptor. Nature 377:748–750; 1995.

Inagami, T. Molecular biology and signaling of angiotensin receptors: an overview. J. Am. Soc. Nephrol. Suppl. 11:S2–S7; 1999.

Ito, M.; Oliverio, M. I.; Mannon, P. J.; Best, C. F.; Maeda, N.; Smithies, O.; Coffman, T. M. Regulation of blood pressure by the type 1A angiotensin II receptor gene. Proc. Natl. Acad. Sci. USA 92:3521–3525; 1995.

Jat, P. S.; Noble, M. D.; Ataliotis, P.; Tanaka, Y.; Yannoutsos, N.; Larsen, L.; Kioussis, D. Direct derivation of conditionally immortal cell lines from an *H-2K*^{b}-tsA58 transgenic mouse. Proc. Natl. Acad. Sci. USA 88:5096–5100; 1991.

Kolb, R. J.; Woost, P. G.; Hopfer, U. Membrane trafficking of angiotensin receptor type-1 and mechanochemical signal transduction in proximal tubule cells. Hypertension 44:352–359; 2004.

Kriz, W.; Knissling, B. Structural organization of the mammalian kidney. In: Seldin, D. W.; Giebisch, G., ed. The kidney: physiology and pathophysiology, Vol. 1, 2nd ed. New York: Raven Press; 1992:707–777.

Lefkowitz, R. J.; Shenoy, S. K. Transduction of receptor signals by β-arrrestins. Science 308:512–517; 2005.

Lin, F.; Cordes, K.; Li, L.; Hood, L.; Couser, W. G.; Shankland, S. J.; Igarashi, P. Hematopoietic stem cells contribute to the regeneration of renal tubules after renal ischemia-reperfusion injury in mice. J. Am. Soc. Nephrol. 14:1188–1199; 2003.

Lutz, M. D.; Cardinal, J.; Burg, M. B. Electrical resistance of renal proximal tubule perfused in vitro. Am. J. Physiol. 225:729–734; 1973.

Marshansky, V.; Bourgoin, S.; Londono, I.; Bendayan, M.; Vinay, P. Identification of ADP-ribosylation factor-6 in brush-border membrane and early endosomes of human kidney proximal tubules. Electrophoresis 18:538–547; 1997.

Morais, C.; Westhuyzen, J.; Pat, B.; Gobe, G.; Healy, H. High ambient glucose is effect neutral on cell death and proliferation in human proximal tubule epithelial cells. Am. J. Physiol. Renal Physiol. 289:F401–F409; 2005.

Muller-Berger, S.; Nesterov, VV.; Fromter, E. Partial recovery of in vivo function by improved incubation conditions of isolated renal proximal tubule. II. Change of Na-HCO_3 cotransport stoichiometry and of response to acetazolamide. Pflugers Arch. 434:383–391; 1997.

Murer, H.; Hernando, N.; Forster, I.; Biber, J. Proximal tubular phosphate reabsorption: molecular mechanisms. Physiol. Rev. 80:1373–1409; 2000.

National Institutes of Health. Public health service policy on humane care and use of laboratory animals. National Institutes of Health: Office of Laboratory Animal Welfare. Bethesda, MD; 2002.

Navar, L. G.; Imig, J. D.; Zou, L.; Wang, C. T. Intrarenal production of angiotensin II. Semin. Nephrol. 17:412–422; 1997.

Nowak, G.; Schnellmann, R. G. Improved culture conditions stimulate gluconeogenesis in primary cultures of renal proximal tubule cells. Am. J. Physiol. 268(4 Pt 1):C1053–C1061; 1995.

Oliverio, M. I.; Coffman, T. M. Angiotensin II receptor physiology using gene targeting. News Physio. Sci. 15:171–175; 2000.

Oliverio, M. I.; Kim, H.-S.; Ito, M., et al. Reduced growth, abnormal kidney structure, and type 2 (AT_2) angiotensin receptor-mediated blood pressure regulation in mice lacking both AT_{1A} and AT_{1B} receptors for angiotensin II. Proc. Natl. Acad. Sci. USA 95:15496–15501; 1998.

Orosz, D. E.; Woost, P. G.; Kolb, R. J., et al. Growth, immortalization, and differentiation potential of normal adult human proximal tubule cells. In Vitro Cell. Dev. Biol. 40A:22–34; 2004.

Pajor, A. M. Molecular properties of sodium/dicarboxylate cotransporters. J. Membrane Biol. 175:1–8; 2000.

Panchapakesan, U.; Sumual, S.; Pollock, C. A.; Chen, X. PPARgamma agonists exert antifibrotic effects in renal tubular cells exposed to high glucose. Am. J. Physiol. Renal Physiol. 289:F1153–F1158; 2005.

Praetorius, H. A.; Frokiaer, J.; Neilsen, S.; Spring, K. R. Bending the primary cilium opens Ca^{2+}-sensitive intermediate-conductance K^+ channels in MDCK cells. J. Membr. Biol. 191:193–200; 2003.

Praetorius, H. A.; Spring, K. R. Bending of the MDCK primary cilium increases intracellular calcium. J. Membr. Biol. 184:71–79; 2001.

Quan, A.; Baum, M. Regulation of proximal tubule transport by endogenously produced angiotensin II. Nephron 84:103–110; 2000.

Romero, M. F.; Douglas, J. G.; Eckert, R. L.; Hopfer, U.; Jacobberger, J. W. Development and characterization of rabbit proximal tubular epithelial cell lines. Kidney Int. 42:1130–1144; 1992.

Scherberich, J. E.; Gauhl, C.; Mondorf, W. Biochemical, immunological and ultrastructural studies on brush-border membranes of human kidney. Curr. Probl. Clin. Biochem. 8:85–95; 1977.

Shenoy, S. K.; Lefkowitz, R. J. Receptor-specific ubiquitination of β-arrestin directs assembly and targeting of seven-transmembrane receptor signalosomes. J. Biol. Chem. 280:15315–15324; 2005.

Todd, J. H.; Sens, M. A.; Hazen-Martin, D. J.; Bylander, J. E.; Smyth, B. J.; Sens, D. A. Variation in the electrical properties of cultured human proximal tubule cells. In Vitro Cell. Dev. Biol. 29A:371–378; 1993.

Touyz, R. M.; Berry, C. Recent advances in angiotensin II signaling. Braz. J. Med. Biol. Res. 35:1001–1015; 2002.

Wolff, M.; Fandrey, J.; Jelkmann, W. Microelectrode measurements of pericellular P_{O2} in erythropoietin-producing human hepatoma cell cultures. Am. J. Physiol. Cell Physiol. 265:C1266–C1270; 1993.

Woost, P. G.; Orosz, D. E.; Jin, W.; Frisa, P. S.; Jacobberger, J. W.; Douglas, J. G.; Hopfer, U. Immortalization and characterization of proximal tubule cells derived from kidneys of spontaneously hypertensive and normotensive rats. Kidney Int. 50:125–134; 1996.

Xu, J.; Li, X. X.; Albrecht, F. E.; Hopfer, U.; Carey, R. M.; Jose, P. A. $Dopamine_1$ receptor, $G_{\alpha o}$, and Na^+-H^+ exchanger interactions in the kidney in hypertension. Hypertension 36:395–399; 2000.

Yeager, T. R.; Reddel, R. R. Constructing immortalized human cell lines. Curr. Opin. Biotech. 10:465–469; 1999.

Yu, P.; Asico, L. D.; Eisner, G. M.; Hopfer, U.; Felder, R. A.; Jose, P. A. Renal protein phosphatase 2A activity and spontaneous hypertension in rats. Hypertension 36:1053–1058; 2000.

Zeng, C.; Asico, L. D.; Wang, X.; Hopfer, U.; Eisner, G. M.; Felder, R. A.; Jose, P. A. Angiotensin II regulation of AT1 and D3 dopamine receptors in renal proximal tubule cells of SHR. Hypertension 41:724–729; 2003a.

Zeng, C.; Luo, Y.; Asico, L. D.; Hopfer, U.; Eisner, G. M.; Felder, R. A.; Jose, P. A. Perturbation of D1 dopamine and AT1 receptor interaction in spontaneously hypertensive rats. Hypertension 42:787–792; 2003b.

Zeng, C.; Wang, D.; Asico, L. D.; Welch, W. J.; Wilcox, C. S.; Hopfer, U.; Eisner, G. M.; Felder, R. A.; Jose, P. A. Aberrant D1 and D3 dopamine receptor transregulation in hypertension. Hypertension 43:654–660; 2004.

Zhu, Z.; Zhang, S. H.; Wagner, C.; Kurtz, A.; Maeda, N.; Coffman, T.; Arendshorst, W. J. Angiotensin AT_{1B} receptor mediates calcium signaling in vascular smooth muscle cells of AT_{1A} receptor-deficient mice. Hypertension 31:1171–1177; 1998.